Noise and Loss in Balanced and Subharmonically Pumped Mixers: Part I—Theory

ANTHONY R. KERR, SENIOR MEMBER, IEEE

Abstract—**In this paper, the theory of noise and frequency conversion is developed for two-diode balanced and subharmonically pumped mixers. Expressions for the conversion loss, noise temperature, and input and output impedances are derived in a form suitable for numerical analysis. Schottky diodes are assumed, having nonlinear capacitance, series resistance (which may be frequency dependent due to skin effect), and shot and thermal noise.**

In Part II, the theory is applied to several practical examples, and computed results are given which show the very different effects of the loop inductance (between the diodes) in balanced and subharmonically pumped mixers. It is also shown that the ideal two-diode mixer using exponential diodes has a multiport noise-equivalent network (attenuator) similar to that of the ideal single-diode mixer.

I. Introduction

FOR MANY years the balanced mixer has been one of the main building blocks of microwave engineering. The inherent symmetry of the balanced mixer gives it two major advantages over the single-ended mixer: 1) down-converted AM noise from the local oscillator (LO) does not appear at the intermediate frequency terminals, and 2) the signal and LO power enter the mixer through separate ports, eliminating the need for an external LO diplexer. In 1974 a new two-diode mixer was reported simultaneously by Schneider and Snell [1], [2] and Cohn *et al.* [3], [4]. This *subharmonically pumped* mixer has the additional advantage of operating with the LO near half the signal frequency, and is particularly attractive at millimeter wavelengths where the cost of local oscillator power increases rapidly with frequency. Work by McMaster *et al.* [5], Carlson *et al.* [6], and Cardiasmenos [7] has demonstrated conversion loss and noise comparable with the best fundamental mixers to over 100 GHz.

In this paper the general loss and noise analysis of single-diode mixers by Held and Kerr [8] is extended to two-diode mixers. The main motivation for this work was the need to understand the effect of two parameters in the design of subharmonically pumped mixers, the loop inductance seen by currents circulating through the two diodes, and the (nonlinear) diode capacitance, both of which have a strong effect on the LO waveforms at the diodes as well as on the small-signal behavior of the mixer.

The small-signal conversion loss and noise properties of a mixer can be determined in two main steps. First, the large-signal voltages and currents produced at the diodes by the LO are determined, and from them the diode conductance and capacitance waveforms. Then, the small-signal conversion loss, input and output impedances, and noise temperature are obtained using linear mixer analysis.

The large-signal waveforms can be determined by computer analysis if the mixer circuit (diode embedding) is known. If the embedding circuit can be represented by a lumped element equivalent circuit, a straightforward time-domain integration of the circuit equations can be performed [9] over a large enough number of LO cycles to allow the steady state to be reached. However, if the mixer contains distributed elements, the embedding circuit is best characterized in the frequency domain, and in this case the nonlinear analysis is more difficult. We have found that harmonic balance techniques [10] will not always converge when a large number (eight to sixteen) of harmonics is considered, although the modified harmonic balance method of Gwarek [11] can be made to converge rapidly in many practical cases provided a suitable combination of parameters can be found for a partial equivalent circuit of the embedding network. However, the multiple-reflection technique described by the author [12] has been found to converge well for all the embedding impedances we have tested, and requires only one arbitrary parameter to be set. This method is directly applicable to two-diode mixers provided the diodes are identical and the embedding network is symmetrical with respect to the diodes.

Having determined the large-signal waveforms at the diodes, the small-signal properties of a two-diode mixer can be deduced using an extension of the theory of conversion developed by Torrey and Whitmer [13].

The theory of shot noise in mixers was first investigated in 1946 by Strutt [14], who showed that to determine the IF output noise of a mixer it was necessary to take into account the correlation of the down-converted components of the periodically varying shot noise of the diode. Following Strutt's original work, the noise in single-diode mixers was studied by several authors [15]–[18] assuming two- or three-frequency models. Uhlir [19] and Dragone [20] performed general analyses of the correlation between the frequency components of periodically varying shot noise in mixers, and this work was applied by Held and Kerr [8], together with an accurate nonlinear analysis and a multifrequency small-signal analysis, to explain the hitherto anomalous noise observed in mixers operating in

Manuscript received March 23, 1979; revised August 8, 1979.
The author is with NASA Goddard Institute for Space Studies, Goddard Space Flight Center, New York, NY 10025.

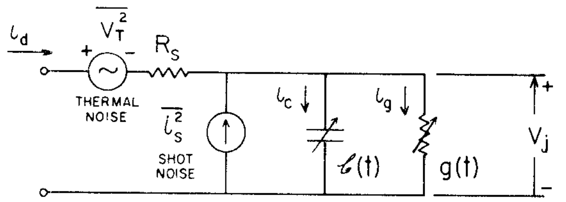

Fig. 1. Equivalent circuit of the Schottky diode, including shot noise due to current flow across the depletion layer, and thermal noise from the series resistance R_s.

the 80–120 GHz region. In the present paper Dragone's noise correlation theory is incorporated in a general small-signal analysis of two-diode mixers.

II. The Pumped Diode

The Schottky diode, now used in almost all microwave mixers, is well represented by the equivalent circuit in Fig. 1, and the analysis in this paper will be based on this model. In high-quality diodes the series resistance R_s may be a function of frequency (due to RF skin-effect) and of voltage (because of depletion layer width modulation), and the capacitance exponent γ may also be voltage dependent. These effects are discussed in [8] and, with the exception of the voltage dependence of R_s, may easily be included in the present analysis. With reference to Fig. 1 we have [21]:

$$i_g = i_0[\exp(\alpha v_j) - 1] \tag{1}$$

$$g = \frac{di_g}{dv_j} = \alpha(i_g + i_0) \tag{2}$$

$$\mathcal{C} = \mathcal{C}_0\left(1 - \frac{v_j}{\phi}\right)^{-\gamma} \tag{3}$$

and

$$i_c = \mathcal{C}\frac{dv_j}{dt} \tag{4}$$

where

$$\alpha = q/\eta kT \tag{5}$$

and the undefined symbols have their usual meanings.

If LO power at frequency ω_p is applied to a diode in a mixer, the resulting periodic conductance and capacitance waveforms will in general contain components at all harmonics of ω_p, and can be written in Fourier series form as

$$g(t) = \sum_{k=-\infty}^{\infty} G_k \exp(jk\omega_p t), \qquad G_{-k} = G_k^* \tag{6}$$

$$\mathcal{C}(t) = \sum_{k=-\infty}^{\infty} C_k \exp(jk\omega_p t), \qquad C_{-k} = C_k^*. \tag{7}$$

For most practical mixers the waveforms $g(t)$ and $\mathcal{C}(t)$ can be determined by computer using the techniques mentioned in the Introduction. The Fourier coefficients G_k and C_k, together with the impedance of the diode mount, govern the small-signal properties of the mixer.

If the mixer operates with an intermediate frequency ω_0, the only small-signal inputs which can generate an IF response are at the sideband frequencies $|\omega_0 + n\omega_p|$, where n is any positive or negative integer. We shall use the concise sideband frequency notation of Saleh [22] in which negative frequencies are used for all lower ($n<0$) sidebands: thus $\omega_n = \omega_0 + n\omega_p$. Writing the small-signal components of the diode voltage and current (v_j and i_d in Fig. 1) at sideband ω_n as δV_n and δI_n, the conversion properties of the pumped diode can be expressed by[1]

$$\boldsymbol{\delta I} = \boldsymbol{Y}\boldsymbol{\delta V} \tag{8}$$

where

$$\boldsymbol{\delta I} = [\cdots, \delta I_1, \delta I_0, \delta I_{-1}, \cdots]^T \tag{9}$$

and

$$\boldsymbol{\delta V} = [\cdots, \delta V_1, \delta V_0, \delta V_{-1}, \cdots]^T. \tag{10}$$

The square matrix $\boldsymbol{Y}$ is the *conversion admittance matrix* of the diode for the particular conductance and capacitance waveforms. For convenience the row and column numbering of all matrices and vectors will correspond to the sideband subscripts. Hence

$$\boldsymbol{Y} \equiv \begin{array}{c} \text{row \#} \\ \vdots \\ 1 \\ 0 \\ -1 \\ \vdots \\ \\ \end{array} \begin{array}{c} \left[\begin{array}{ccccc} & \vdots & \vdots & \vdots & \\ \cdots & Y_{11} & Y_{10} & Y_{1-1} & \cdots \\ \cdots & Y_{01} & Y_{00} & Y_{0-1} & \cdots \\ \cdots & Y_{-11} & Y_{-10} & Y_{-1-1} & \cdots \\ & \vdots & \vdots & \vdots & \end{array}\right] \\ \begin{array}{ccccc} \cdots & 1 & 0 & -1 & \cdots \end{array} \\ \text{column \#} \end{array} \tag{11}$$

Using this notation the elements of $\boldsymbol{Y}$ are given by [13]

$$Y_{mn} = G_{m-n} + j\omega_m C_{m-n} \tag{12}$$

where G_k and C_k are the Fourier coefficients of the diode conductance and capacitance as defined in (6) and (7).

The admittance matrix $\boldsymbol{Y}$ allows the pumped diode to be characterized for small-signal analysis as a (multifrequency) multiport network with one port for each sideband frequency ω_n.

III. Two-Diode Mixer Small-Signal Analysis

In Fig. 2 two pumped diodes are shown connected via their mount to external sources and loads at the various sideband frequencies ω_k. In the previous section the pumped diode was characterized for small-signal analysis by a multifrequency multiport network with admittance matrix $\boldsymbol{Y}$. It follows that two diodes and their mount can be represented as three interconnected networks as shown in Fig. 3. Note that the embedding network defined in Fig. 3 includes the diode mount, the series resistance of the diodes, and all source and load admittances Y_k connected externally to the mount in Fig. 2, so that *in normal operation all the ports shown in Fig. 3 are either open-circuited or connected to current sources at appropriate*

[1] A superscript T indicates the transpose of a vector or matrix.

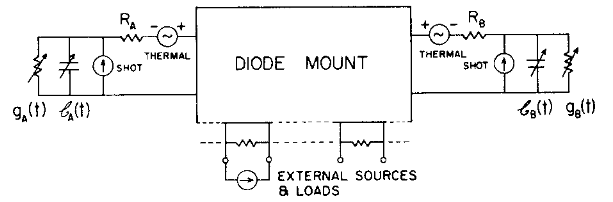

Fig. 2. Circuit of the two-diode mixer.

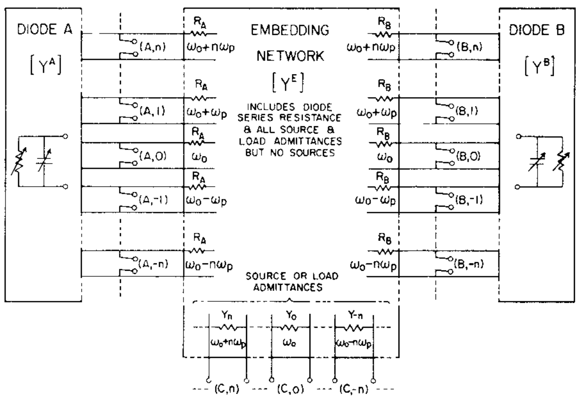

Fig. 3. Representation of the mixer as a multifrequency multiport network. The embedding network contains the series resistance of the diodes and all source and load admittances Y_k connected externally to the diode mount. In normal mixer operation the ports shown in this diagram are all either open-circuited or connected to current sources at appropriate sideband frequencies. Port numbering (X,k) is such that $X(=A,B,\text{or } C)$ indicates one of three faces of the embedding network, and k indicates sideband frequency $\omega_k = \omega_0 + k\omega_p$.

sideband frequencies. For clarity a double-index port numbering system is used (e.g., $(A,-1)$) in which the first index is a letter (A,B, or C) denoting one of three faces of the embedding network, and the second index is a positive or negative integer k corresponding to the sideband frequency ω_k of the port. On each of the three faces there is one port for each sideband. The embedding network has the admittance matrix $\boldsymbol{Y}^E$, a typical element of which is $Y^E_{(A,m)(B,n)}$. Row and column numbering of $\boldsymbol{Y}^E$ is as follows:

$$\begin{array}{c}A,N\\ \vdots\\ A,0\\ \vdots\\ A,-N\\ B,N\\ \vdots\\ B,0\\ \vdots\\ B,-N\\ C,N\\ \vdots\\ C,0\\ \vdots\\ C,-N\end{array}\left[\begin{array}{c|c|c} \quad & \quad & \quad \\ \hline \quad & \quad & \quad \\ \hline \quad & \quad & \quad \end{array}\right]$$

$$(A,N)\cdots(A,0)\cdots(A,-N) \quad (B,N)\cdots(B,0)\cdots(B,-N) \quad (C,N)\cdots(C,0)\cdots(C,-N)$$

Since the embedding network is linear and time-invariant there is no internal coupling between ports at different sideband frequencies, and hence the only nonzero elements of $\boldsymbol{Y}^E$ are those for which $m=n$.

Partitioning $\boldsymbol{Y}^E$ into nine equal-sized submatrices gives

$$\boldsymbol{Y}^E = \left[\begin{array}{c|c|c} Y^E_{AA} & Y^E_{AB} & Y^E_{AC} \\ \hline Y^E_{BA} & Y^E_{BB} & Y^E_{BC} \\ \hline Y^E_{CA} & Y^E_{CB} & Y^E_{CC} \end{array}\right] \tag{13}$$

where the submatrices are all diagonal matrices (off-diagonal elements are zero).

If the conversion admittance matrices (8) of the two pumped diodes are denoted by $\boldsymbol{Y}^A$ and $\boldsymbol{Y}^B$, the parallel connection of the two diodes with the embedding network, as shown in Fig. 3, results in an overall *mixer admittance matrix*

$$\boldsymbol{Y}^M = \left[\begin{array}{c|c|c} Y^A + Y^E_{AA} & Y^E_{AB} & Y^E_{AC} \\ \hline Y^E_{BA} & Y^B + Y^E_{BB} & Y^E_{BC} \\ \hline Y^E_{CA} & Y^E_{CB} & Y^E_{CC} \end{array}\right]. \tag{14}$$

All the small-signal properties of the mixer can be derived from this matrix and the source and load admittances Y_k.

A. Output Impedance

To determine the IF output impedance of the mixer, the IF load admittance Y_0 (considered here as part of the embedding network, as shown in Fig. 3) is set to zero, so the impedance seen looking into port $(C,0)$ is simply the output impedance. Let $\boldsymbol{Y}^{Mo/c}$ denote the admittance matrix of the mixer with zero load admittance, and define

$$\boldsymbol{Z}^{Mo/c} \triangleq (\boldsymbol{Y}^{Mo/c})^{-1}. \tag{15}$$

The output impedance of the mixer is given by element $(C,0)(C,0)$ of $\boldsymbol{Z}^{Mo/c}$; i.e.,

$$Z_{\text{out}} = Z^{Mo/c}_{(C,0)(C,0)}. \tag{16}$$

For optimum conversion loss the output of the mixer should be conjugate-matched, which is achieved if the IF load admittance

$$Y_0 = 1/\left(Z^{M\,o/c}_{(C,0)(C,0)}\right)^*. \tag{17}$$

B. Conversion Loss

Inverting the mixer admittance matrix gives the mixer impedance matrix

$$\boldsymbol{Z}^M \triangleq (\boldsymbol{Y}^M)^{-1}. \tag{18}$$

If a small test current $\delta I_{(C,k)}$ at sideband ω_k is applied at port (C,k) of the mixer, the IF response at port $(C,0)$ is

$$\delta V_{(C,0)} = Z^M_{(C,0)(C,k)} \delta I_{(C,k)}. \tag{19}$$

The power delivered to the IF load is $|\delta V_{(C,0)}|^2 \mathrm{Re}[Y_0]$, and the power available from the source is $|\delta I_{(C,k)}|^2 / 4\,\mathrm{Re}[Y_k]$. Hence the conversion loss from sideband ω_k to the IF ω_0 is

$$L_{0,k} = \frac{1}{4|Z^M_{(C,0)(C,k)}|^2 \mathrm{Re}[Y_k]\,\mathrm{Re}[Y_0]}. \tag{20}$$

In a similar way it is possible to determine the conversion loss between any two sidebands.

C. Input Impedance

The impedance $Z_{\mathrm{port}(C,k)}$ looking into the ω_k port(C,k) on face C of the embedding network (Fig. 3) is given by the appropriate element of the mixer impedance matrix $\boldsymbol{Z}^M$ defined in (18):

$$Z_{\mathrm{port}(C,k)} = Z^M_{(C,k)(C,k)}. \tag{21}$$

$Z_{\mathrm{port}(C,k)}$ is the impedance of the parallel combination of the source admittance Y_k and the mixer itself. The actual input impedance of the mixer is the impedance seen by the source admittance, and is, therefore,

$$Z_{in_k} = \left(\frac{1}{Z^M_{(C,k)(C,k)}} - Y_k \right)^{-1}. \tag{22}$$

IV. Noise

The analysis of noise in a mixer is performed in two steps: First, the equivalent noise generators and their correlation properties are determined for shot noise in the pumped diodes and for thermal noise in the diode series resistance and diode mount. Then these equivalent generators are connected to the mixer to determine the IF output noise.

A. Shot Noise

The equivalent circuit of the Schottky diode, including noise sources, is shown in Fig. 1. For a dc-biased diode the shot noise is Gaussian, with mean-square amplitude given by the usual equation:

$$\overline{i_s^2} = 2qi_g\Delta f. \tag{23}$$

When the diode is pumped at frequency ω_p by the local oscillator, the current in the conductance can be written in Fourier series form as

$$i_g(t) = \sum_{n=-\infty}^{\infty} I_n \exp(jn\omega_p t), \qquad I_{-n} = I_n^*. \tag{24}$$

As suggested by (23) and (24), the shot noise of the pumped diode can be considered as periodically amplitude modulated Gaussian noise. Following the method of Dragone [20], the *unmodulated* Gaussian noise can be regarded as a multitude of pseudosinusoidal components [23], [24] with different frequencies and random amplitudes and phases; the effect of the modulation is to generate sideband components related in amplitude and phase to each of the original pseudosinusoids. When observed with finite bandwidth, the noise character of the signal is preserved because of the large number of pseudosinusoids with different frequencies. For the pumped diode let δI_{S_m} and δI_{S_n} denote the complex amplitudes of pseudosinusoidal components of the shot noise at sidebands ω_m and ω_n. Dragone has shown that the correlation between the shot noise at ω_m and ω_n is

$$\langle \delta I_{S_m} \delta I_{S_n}^* \rangle = 2qI_{m-n}\Delta f \tag{25a}$$

where $\langle \text{- - -} \rangle$ denotes the statistical (or ensemble) average, and I_{m-n} is a Fourier component of $i_g(t)$, as defined in (24).

When two pumped diodes are considered, the shot noise in each can likewise be regarded as amplitude modulated Gaussian noise. Clearly there is no correlation between the *unmodulated* noise of the two diodes since their physical processes of noise generation are completely independent. The modulation process generates additional (correlated) sideband components at each diode; however, since there is no correlation between the pseudosinusoidal components of their unmodulated noise, there will be no correlation between their modulated noise. For the two-diode mixer we shall use superscripts A and B to distinguish between the diodes connected at faces A and B of the embedding network (Fig. 3); thus it follows that

$$\left.\begin{aligned} \langle \delta I^A_{S_m}\, \delta I^{A*}_{S_n} \rangle &= 2qI^A_{m-n}\Delta f \\ \langle \delta I^B_{S_m}\, \delta I^{B*}_{S_n} \rangle &= 2qI^B_{m-n}\Delta f \\ \langle \delta I^A_{S_m}\, \delta I^{B*}_{S_n} \rangle &= 0. \end{aligned}\right\}. \tag{25b}$$

B. Thermal Noise

Any linear network containing sources can be represented by a Norton equivalent circuit consisting of the source-less network[2] with a current source connected at each port. Each current source is equal to the short-circuit current at the same port of the original network when all other ports are short-circuited. For a lossy reciprocal N-port network at temperature T, let the pseudosinusoidal short-circuit thermal noise currents at the ports, at any frequency ω, be δI_{T_n}, $n = 1, \cdots, N$. It has been shown by

[2] Current sources in the original network are replaced by open-circuits, voltage sources by short-circuits.

Twiss [25] that

$$\langle \delta I_{T_m} \delta I_{T_n}^* \rangle = 4kT\mathrm{Re}[Y_{mn}]\Delta f \tag{26}$$

where Y_{mn} is an element of the admittance matrix of the network.

The embedding network of the two-diode mixer, as defined in Fig. 3, contains the series resistance of the diodes and also the source and load admittances normally connected externally to the mixer. In characterizing the mixer's noise performance, the external terminations should be considered noiseless. It is therefore expedient to regard the embedding network as composed of two parallel connected subnetworks, one at temperature T, and the other, containing only the external terminations, at absolute zero temperature. If the admittance matrices of these subnetworks are respectively $\boldsymbol{Y}^{E(\text{unterm.})}$ and $\boldsymbol{Y}^{\text{term}}$, then

$$\boldsymbol{Y}^E = \boldsymbol{Y}^{E(\text{unterm.})} + \boldsymbol{Y}^{\text{term.}}. \tag{27}$$

It is now possible to apply (26) to the two subnetworks separately.[3] Since $\boldsymbol{Y}^{\text{term.}}$ at zero temperature contributes nothing to (26),

$$\langle \delta_{T(X,m)} \delta I_{T(Y,n)}^* \rangle = 4kT\mathrm{Re}[Y_{(X,m)(Y,n)}^{E\,(\text{unterm.})}]\Delta f \tag{28}$$

where (X,m) and (Y,n) are any of the ports defined in Fig. 3.

C. Input Noise Temperature

To determine the equivalent input noise temperature of the two-diode mixer we first determine the IF output noise power due to shot and thermal noise. Equations (25) and (28) give the correlation properties of the equivalent shot and thermal noise current sources which, in the complete mixer (Fig. 3), are connected to each of the ports. If the pseudosinusoidal noise current source at port (X,k) is $\delta I_{N_{(X,k)}}$, we can form a vector of all the input noise currents:

$$\boldsymbol{\delta I}_N = [\ldots, \delta I_{N_{(A,1)}}, \delta I_{N_{(A,0)}}, \delta I_{N_{(A,-1)}}, \ldots \delta I_{N_{(B,1)}}, \delta I_{N_{(B,0)}}, \delta I_{N_{(B,-1)}} \ldots, \delta I_{N_{(C,1)}}, \delta I_{N_{(C,0)}}, \delta I_{N_{(C,-1)}}, \ldots]^T \tag{29a}$$

where

$$\begin{aligned} \delta I_{N_{(A,k)}} &= \delta I_{S_k}^A + \delta I_{T_{(A,k)}} \\ \delta I_{N_{(B,k)}} &= \delta I_{S_k}^B + \delta I_{T_{(B,k)}} \\ \delta I_{N_{(C,k)}} &= \delta I_{T_{(C,k)}}. \end{aligned} \tag{29b}$$

Likewise denoting the port noise voltages by $\delta V_{N_{(X,k)}}$ we have

$$\begin{aligned} \boldsymbol{\delta V}_N = [&\cdots, \delta V_{N_{(A,1)}}, \delta V_{N_{(A,0)}}, \delta V_{N_{(A,-1)}}, \cdots, \\ &\delta V_{N_{(B,1)}}, \delta V_{N_{(B,0)}}, \delta V_{N_{(B,-1)}}, \cdots, \\ &\delta V_{N_{(C,1)}}, \delta V_{N_{(C,0)}}, \delta V_{N_{(C,-1)}}, \cdots]^T. \end{aligned} \tag{30}$$

[3] The fact that these networks are *multifrequency* multiport networks does not invalidate the use of (26): clearly, if the noise currents δI_m and δI_n are at the same sideband frequency, (26) is applicable. When the currents are at different sideband frequencies the corresponding elements of $\boldsymbol{Y}^E$ are zero, giving, via (26), zero correlation between the different sideband noise current components. This is the expected result for a linear time-invariant network.

From the definition (14) of the mixer admittance matrix it follows that

$$\boldsymbol{\delta I}_N = \boldsymbol{Y}^M \boldsymbol{\delta V}_N. \tag{31}$$

Solving for $\boldsymbol{\delta V}_N$ gives

$$\boldsymbol{\delta V}_N = \boldsymbol{Z}^M \boldsymbol{\delta I}_N \tag{32}$$

where $\boldsymbol{Z}^M = (\boldsymbol{Y}^M)^{-1}$. Postmultiplying (32) by its own conjugate transpose gives[4]

$$\boldsymbol{\delta V}_N \boldsymbol{\delta V}_N^\dagger = \boldsymbol{Z}^M \boldsymbol{\delta I}_N \boldsymbol{\delta I}_N^\dagger \boldsymbol{Z}^{M^\dagger} \tag{33}$$

from which it follows that

$$\delta V_{N_{(C,0)}} \delta V_{N_{(C,0)}}^* = \boldsymbol{Z}_{(C,0)}^M \boldsymbol{\delta I}_N \boldsymbol{\delta I}_N^\dagger \boldsymbol{Z}_{(C,0)}^{M^\dagger} \tag{34}$$

where $\boldsymbol{Z}_{(C,0)}^M$ is the $(C,0)$ row of matrix $\boldsymbol{Z}^M$. $\delta V_{N_{(C,0)}}$ is the IF output voltage appearing at the output port $(C,0)$ of the mixer. Taking the ensemble average in (34) give the mean-square IF output noise voltage

$$\langle \delta V_{N_{(C,0)}} \delta V_{N_{(C,0)}}^* \rangle = \boldsymbol{Z}_{(C,0)}^M \langle \boldsymbol{\delta I}_N \boldsymbol{\delta I}_N^\dagger \rangle \boldsymbol{Z}_{(C,0)}^{M^\dagger}. \tag{35}$$

The square matrix $\boldsymbol{N} \triangleq \langle \boldsymbol{\delta I}_N \boldsymbol{\delta I}_N^\dagger \rangle$ is the *noise current correlation matrix* for the mixer and has the general element $N_{(X,m)(Y,n)} = \langle \delta I_{N_{(X,m)}} \delta I_{N_{(Y,n)}}^* \rangle$ where (X,m) and (Y,n) are any port numbers of the mixer. From (25), (28), and (29) it follows that, since the shot and thermal processes are completely independent,

$$N_{(A,m)(A,n)} = 2qI_{m-n}^A \Delta f + 4kT\mathrm{Re}[Y_{(A,m)(A,n)}^{E\,(\text{unterm.})}]\Delta f \tag{36a}$$

$$N_{(B,m)(B,n)} = 2qI_{m-n}^B \Delta f + 4kT\mathrm{Re}[Y_{(B,m)(B,n)}^{E\,(\text{unterm.})}]\Delta f \tag{36b}$$

and, for all other combinations of values (A, B, or C) of X and Y,

$$N_{(X,m)(Y,n)} = 4kT\mathrm{Re}[Y_{(X,m)(Y,n)}^{E\,(\text{unterm.})}]\Delta f. \tag{36c}$$

The noise power delivered to the IF load admittance Y_0 is then

$$P = \boldsymbol{Z}_{(C,0)}^M \boldsymbol{N} \boldsymbol{Z}_{(C,0)}^{M^\dagger} \cdot \mathrm{Re}[Y_0]. \tag{37}$$

Multiplying by the conversion loss (20) gives the noise power $PL_{0,n}$ which must be available from a noisy source admittance Y_n at sideband ω_n to produce the same power in the IF load as the mixer itself. The equivalent temperature of Y_n is the (single-sideband) noise temperature T_M of the mixer, and is given (using (20)) by

$$\begin{aligned} T_M &= PL_{0,n}/k\Delta f \\ &= \frac{\boldsymbol{Z}_{(C,0)}^M \boldsymbol{N} \boldsymbol{Z}_{(C,0)}^{M^\dagger}}{4k\mathrm{Re}[Y_n] \cdot |Z_{(C,0)(C,n)}^M|^2 \Delta f}. \end{aligned} \tag{38}$$

V. Discussion

The small-signal and noise theory of two-diode mixers, given in Sections III and IV, is generally applicable to balanced or subharmonically pumped mixers having two diodes mounted in any circuit. The diodes need not be

[4] A superscript $\dagger$ denotes the conjugate transpose of a matrix or vector.

identical, and the mount may be lossy and need not be symmetrical. When skin-effect is present in the diodes the series resistance should be considered a function of frequency and the elements of the admittance matrix $\boldsymbol{Y}^E$ modified accordingly.

In the analysis no distinction has been made between balanced and subharmonically pumped mixers. The difference lies only in the internal structure of the embedding network, which governs the relative phasing of the diodes with respect to the external ports at the various sideband frequencies and pump harmonics.

To perform the small-signal and noise analysis, the large-signal diode conductance and capacitance waveforms produced by the LO must be determined. As mentioned in the Introduction, this can be achieved using existing techniques when the embedding network is symmetrical and the diodes are identical. For cases with dissimilar diodes and/or asymmetrical embedding networks, a new method must be developed for the nonlinear analysis. It would appear possible to extend the method used [12] for single-diode and symmetrical two-diode mixers to cover the more general case, although we have not attempted this.

Extension of the present analysis to mixers with more than two diodes is straightforward. The embedding network of Fig. 3 requires an additional set of ports for each additional diode, and the matrices $\boldsymbol{Y}^M$ and $\boldsymbol{Z}^M$ must be enlarged correspondingly. Otherwise the analysis remains unchanged.

In part II of this paper the theory of two-diode mixers is applied to specific examples and computed results are given. It is also shown that the noise of an ideal two-diode mixer, having exponential diodes without series resistance or nonlinear capacitance, is equivalent to that of a lossy network at temperature $\eta T/2$, thus answering the question of whether a subharmonically pumped resistive mixer is inherently less noisy than a fundamental resistive mixer.

References

[1] M. V. Schneider and W. W. Snell, "Stripline downconverter with subharmonic pump," *Bell Syst. Tech. J.*, vol. 53, no. 6, pp. 1179–1183, July–Aug. 1974.

[2] ——, "Harmonically pumped stripline down-converter," *IEEE Trans. Microwave Theory Tech.*, vol. MTT-23, pp. 271–275, Mar. 1975.

[3] M. Cohn, J. E. Degenford, and B. A. Newman, "Harmonic mixing with an antiparallel diode pair," 1974 *MTT Int. Symp. Dig.*, pp. 171–172, June 12–14, 1974.

[4] ——, *IEEE Trans. Microwave Theory Tech.*, vol. MTT-23, pp. 667–673, Aug. 1975.

[5] T. F. McMaster, M. V. Schneider, and W. W. Snell, "Millimeter-wave receivers with subharmonic pump," *IEEE Trans. Microwave Theory Tech.*, vol. MTT-24, pp. 948–952, Dec. 1976.

[6] E. R. Carlson, M. V. Schneider, and T. F. McMaster, "Subharmonically pumped millimeter-wave mixers," *IEEE Trans. Microwave Theory Tech.*, vol. MTT-26, pp. 706–715, Oct. 1978.

[7] A. G. Cardiasmenos, "Low-noise thin-film downconverters for millimeter systems applications," in 1978 *IEEE MTT-S Int. Microwave Symp. Dig.*, pp. 399–401, June 27–29, 1978.

[8] D. N. Held and A. R. Kerr, "Conversion loss and noise of microwave and millimeter-wave mixers: Part 1—Theory," and "Part 2—Experiment," *IEEE Trans. Microwave Theory Tech.*, vol. MTT-26, pp. 49–61, Feb. 1978.

[9] D. A. Fleri and L. D. Cohen, "Nonlinear analysis of the Schottky-barrier mixer diode," *IEEE Trans. Microwave Theory Tech.*, vol. MTT-21, pp. 39–43, Jan. 1973.

[10] S. Egami, "Nonlinear, linear analysis and computer-aided design of resistive mixer," *IEEE Trans. Microwave Theory Tech.*, vol. MTT-22, pp. 270–275, Mar. 1974.

[11] W. K. Gwarek, "Nonlinear analysis of microwave mixers," M. S. thesis, *Massachusetts Inst. Technol.*, Cambridge, MA, Sept. 1974.

[12] A. R. Kerr, "A technique for determining the local oscillator waveforms in a microwave mixer," *IEEE Trans. Microwave Theory Tech.*, vol. MTT-23, pp. 828–831, Oct. 1975.

[13] H. C. Torrey and C. A. Whitmer *Crystal Rectifiers* (M.I.T. Radiation Lab. Series, vol. 15). New York: McGraw-Hill, 1948.

[14] M. J. O. Strutt, "Noise-figure reduction in mixer stages," *Proc. IRE*, vol. 34, no. 12, pp. 942–950, Dec. 1946.

[15] A. van der Ziel and R. L. Watters, "Noise in mixer tubes," *in Proc. IRE*, vol. 46, pp. 1426–1427, 1958.

[16] A. van der Ziel, *Noise: Sources, Characterization, and Measurement.* Englewood Cliffs, NJ: Prentice-Hall, 1970.

[17] C. S. Kim, "Tunnel diode converter analysis," *IRE Trans. Electron Devices*, vol. ED-8, pp. 394–405, Sept. 1961.

[18] C. A. Liechti, "Down-converters using Schottky-barrier diodes," *IEEE Trans. Electron Devices*, vol. ED-17, pp. 975–983, Nov. 1970.

[19] A. Uhlir, Jr., "Shot noise in p-n junction frequency converters," *Bell Syst. Tech. J.* vol. 37, pp. 951–988, July 1958.

[20] C. Dragone, "Analysis of thermal and shot noise in pumped resistive diodes," *Bell Syst. Tech. J.*, vol. 47, pp. 1883–1902, Nov. 1968.

[21] S. M. Sze, *Physics of Semiconductor Devices*, New York: Wiley 1969.

[22] A. A. M. Saleh, *Theory of Resistive Mixers.*, Cambridge, MA: M.I.T. Press, 1971.

[23] S. O. Rice, "Mathematical analysis of random noise," *Bell Syst. Tech. J.*, vol. 23, no. 3, pp. 282–332, July 1944.

[24] W. R. Bennet, *Electrical Noise.* New York: McGraw-Hill, 1960.

[25] R. Q. Twiss, "Nyquist's and Thevenin's theorems generalized for nonreciprocal linear networks," *J. Appl. Phys.*, vol. 26, no. 5, pp. 599–602, May 1955. See also E. J. Schremp in ch. 12 of "Vacuum Tube Amplifiers," G. E. Valley and H. Wallman, Eds. (vol. 18 of M.I.T. Radiation Lab. Series), New York: McGraw-Hill, 1948.